Laboratory Investigation (2021) 101:1036–1047
https://doi.org/10.1038/s41374-021-00590-w

ARTICLE

Early response in phosphorylation of ribosomal protein S6 is associated with sensitivity to trametinib in colorectal cancer cells

Yuka Hirashita[1,2] · Yoshiyuki Tsukamoto[2] · Yoko Kudo[1] · Daisuke Kakisako[1] · Shusaku Kurogi[2] · Naoki Hijiya[2] · Chisato Nakada[2] · Tomohisa Uchida[2] · Teijiro Hirashita[3] · Takahiro Hiratsuka[3] · Tomonori Akagi[3] · Yoshitake Ueda[4] · Hidefumi Shiroshita[3] · Tsuyoshi Etoh[3] · Kazuhiro Mizukami[1] · Koichi Honda[1] · Tadayoshi Okimoto[1] · Masaaki Kodama[1] · Masafumi Inomata[3] · Masatsugu Moriyama[2] · Kazunari Murakami[1]

Received: 27 June 2020 / Revised: 8 March 2021 / Accepted: 9 March 2021 / Published online: 28 April 2021

Abstract

Mutations in RAS or BRAF are associated with poor prognosis and resistance to epidermal growth factor receptor (EGFR)-targeted therapy in colorectal cancer (CRC). Despite their common ability to activate downstream genes such as MEK and ERK, the therapeutic benefit of MEK inhibitors for patients with RAS/BRAF mutant CRC is limited, highlighting the need for biomarkers to predict the efficacy of MEK inhibition. Previously, we reported that a change in phosphorylation of ribosomal protein S6 (pS6) after MEK inhibition was significantly associated with sensitivity to MEK inhibition in gastric cancer cells. Here, we investigated the value of the response in pS6 for predicting the efficacy of trametinib, a MEK inhibitor, in patients with RAS/BRAF mutant CRC using patient-derived CRC organoids. We found that a subset of CRC cell lines and organoids were sensitive to trametinib. The change in phosphorylated ERK, a downstream molecule of the RAS/RAF/MEK pathway, was not significantly associated with trametinib sensitivity. On the other hand, only those with sensitivity showed a reduction of pS6 levels in response to trametinib. The change in pS6 after trametinib treatment was detectable by Western blotting, immunohistochemistry or immunocytochemistry. We also demonstrated an impact of MEK inhibition on pS6 in vivo using a xenograft model. Our data suggest that, in combination with patient-derived organoids, immunostaining-based detection of pS6 could be useful for prediction of trametinib sensitivity.

Introduction

The survival benefit of chemotherapy with traditional cytotoxic agents is only limited. The relatively new approach of molecular targeted therapy, whereby treatment is optimized on the basis of genomic alterations in individuals [1–3], has yielded new opportunities for cancer treatment. However, methods that can predict the effectiveness of these molecular targeting agents are still limited.

Previously, we have identified that a change in the phosphorylation of ribosomal protein S6 (pS6) in response to MEK inhibition can be used as a predictive biomarker for MEK inhibition in gastric cancer (GC), which is characterized by alterations in receptor tyrosine kinase (RTK)/KRAS. We found that this biomarker was more significantly associated with sensitivity to MEK inhibition than genomic alterations of RTK/KRAS in GC cells [4]. Although this type of predictive biomarker would be potentially useful for diagnosis, it is currently difficult to obtain paired clinical tissue samples taken before and after

Supplementary information The online version contains supplementary material available at https://doi.org/10.1038/s41374-021-00590-w.

✉ Yuka Hirashita
not-minamino@oita-u.ac.jp

✉ Yoshiyuki Tsukamoto
tuka@oita-u.ac.jp

[1] Department of Gastroenterology, Faculty of Medicine, Oita University, Oita, Japan

[2] Department of Molecular Pathology, Faculty of Medicine, Oita University, Oita, Japan

[3] Department of Gastroenterological and Pediatric Surgery, Faculty of Medicine, Oita University, Oita, Japan

[4] Department of Comprehensive Surgery for Community Medicine, Oita University, Oita, Japan

drug treatment due to ethical issues, including unacceptable invasiveness to patients. The recent development of 3D culture systems has enabled us to establish organoids derived from cancer patients and upscale them to screen for drug efficacy without the need for clinical administration to patients [5–8].

In addition to conventional chemotherapies, epidermal growth factor receptor (EGFR)-targeted therapies have been applied successfully for patients with colorectal cancer (CRC) [9]. However, CRC patients with RAS or BRAF mutation are currently excluded from EGFR-targeted therapy because these mutant proteins activate downstream of the EGFR independently from EGFR activation [10, 11]. This suggests that sustained activation of the RAS downstream signaling pathway is pivotal for CRC cells. Although it was expected that a MEK inhibitor capable of inhibiting the RAS/MEK/ERK signaling pathway would be effective for CRC patients currently excluded from EGFR-targeted therapy, clinical trials involving patients with RAS-mutated CRC revealed no superiority of MEK inhibitors in comparison with conventional chemotherapies [12–14]. Therefore, to demonstrate the true clinical benefits of MEK inhibitors, novel diagnostic methods with reliable predictive biomarkers are needed.

In the present study using CRC patient-derived organoids, we evaluated the potential application of the change in pS6 as a predictive biomarker of MEK inhibition to discriminate patients with high sensitivity to MEK inhibition.

Materials and methods

Cell lines

CRC cell lines were obtained from RIKEN Bio Resource Center (COLO-205, COLO-320, CW-2 and HCT 116; Ibaraki, Japan) or the Korean Cell Line Bank (SNU-1033, SNU-C2A and SNU-C5; Seoul, Korea). They were maintained in RPMI (COLO-205, COLO-320, CW-2, SNU-1033, SNU-C2A, and SUN-C5) or DMEM (HCT-116) supplemented with 10% fetal bovine serum (FBS).

Establishment of patient-derived tumor organoids

Establishment of organoids from CRCs was approved by all the patients concerned and by the Oita University Ethics Committee (Approval No 1541). Clinicopathological information about the patients with CRC is provided in Table 1. Organoids were established as reported previously by other groups with some modifications [5, 15]. CRC tissues from surgical specimens (~30 mm^3) or from endoscopic biopsy samples (~10 mm^3) were minced into 0.5 mm^3 fragments using scalpels and washed three times with cold wash medium (DMEM (Thermo Fisher Scientific, Waltham, MA, USA)) supplemented with 1% FBS and 1% penicillin/streptomycin (Thermo Fisher Scientific). Then, the tissue fragments were incubated in a digestion solution containing 0.125 mg/ml collagenase XI (Sigma-Aldrich, Irvine, UK) and 0.125 mg/ml dispase II (Thermo Fisher Scientific) in wash medium, at 37 °C for 40 min with shaking. After the remaining tissue fragments had settled under gravity, the resulting supernatant was transferred to a new 15 ml tube and centrifuged at 4 °C 300 × *g* for 20 min. The collected tumor cells were embedded in a 1:3 mixture of wash medium and growth factor-reduced Corning Matrigel (Falcon, Corning, NY, USA) and placed as 20 µl droplets in a multi-well plate. They were then overlaid with organoid culture medium comprising the following components: Advanced DMEM (Thermo Fisher Scientific) with 20% R-spondin-conditioned medium (Trevigen, Gaithersburg, MD, USA), 10% noggin-conditioned medium (MTA for the producer cell line was obtained from the Hubrecht Institute, the Netherlands), 1 × B27 (Thermo Fisher Scientific), 1.25 mM n-acetyl cysteine (Sigma-Aldrich), 10 mM nicotinamide (Sigma-Aldrich), 50 ng/ml recombinant human EGF (PeproTech, London, UK), 500 nM A83-01 (R&D Systems, Minneapolis, Minnesota, USA), 3 µM SB202190 (Sigma-Aldrich), 1 µM prostaglandin E2 (Tocris, Bioscience, Bristol, UK) and 100 µg/ml primocin (InvivoGen, San Diego, CA, USA). The medium was refreshed every 2 days. For passage, organoids were collected in a new 15 ml tube and broken up by pipetting with flame-narrowed Pasteur pipets. They were then suspended in 10 ml of wash medium, and spun down at 4 °C 300 × *g* for 5 min. Each pellet was reseeded as described above at a passaging ratio of 1:2–1:4 depending on growth speed.

Table 1 Information for cancer tissue specimens obtained from CRC patients.

	Age	Sex	Location	Stage[a]	Differentiation[a]
C1	58	M	Ascending	IIa	Moderately
C2	67	M	Rectum (Rb)	IIIb	Well
C3	83	F	Ascending	IVa	Well
C5	90	M	Ascending	IIa	Moderately
C6	65	M	Ascending	IIIb	Moderately
C7	77	M	Rectum (Ra)	IIIb	Well
C9	80	F	Ascending	I	Moderately
C10	84	M	Ascending	I	Well
C13	85	M	Sigmoid	II	Moderately
C16	89	F	Ascending	IVa	Well

[a]Japan society for cancer of the colon and rectum. Japanese classification of colorectal, appendiceal, and anal carcinoma, 3rd English edition; Kanehara & Co, Ltd.

Table 2 Primer sequences for quantitative PCR and sequencing.

Gene	Exon	Primer Sequence (5′-3′)	Product size (bp)
KRAS	**2**	F: AAAGGTACTGGTGGAGTATTTGATAG R: AAACCCAAGGTACATTTCAGATAAC	**349**
KRAS	**3**	F: CAGGATTCCTACAGGAAGCAAGTAG R: CACAAAGAAAGCCCTCCCCA	**133**
KRAS	**4**	F: TGACAAAAGTTGTGGACAGGT R: AAGAAGCAATGCCCTCTCAA	**388**
NRAS	**2**	F: TGGAAGGTCACACTAGGGTTTT R: TGGGTAAAGATGATCCGACA	**288**
NRAS	**3**	F: TCTTACAGAAAACAAGTGGT R: GTAGAGGTTAATATCCGCAA	**174**
HRAS	**4**	F: GCCTAATCTTGTTTTTCTTATGTTCTG R: TGAATATGGATCACATCTCTACCAG	**285**
BRAF	**15**	F: TCATAATGCTTGCTCTGATAGGA R: GGCCAAAAATTTAATCAGTGGA	**214**

Mutation analysis of the RAS (exons 2, 3 and 4) and BRAF (exon 15) genes

Genomic DNA from organoids was amplified and sequenced using the primers listed in Table 2. TaKaRa Ex Tag (Takara Bio, Shiga, Japan) and a BigDye Terminator v3.1 cycle sequencing kit (Applied Biosystem, Foster City, CA, USA) were used for PCR and sequencing, respectively, in accordance with the manufacturers' instructions.

Cell line viability assay

Cells were seeded at a density of $1.6–3.2 \times 10^3$ cells/well in 96-well plates, depending on their growth speed to reach subconfluency at 96 h after plating. They were incubated for 24 h and then treated with DMSO or serially diluted trametinib (0.01, 0.1, 1.0 and 10 μM) (ChemScene, Monmouth Junction, NJ, USA) or PD0325901 (0.01, 0.1, 1.0 and 10 μM) (LC Laboratories, Woburn, MA, USA) for 72 h. The growth-inhibitory effect of the trametinib was analyzed by CellTiter96 aqueous one solution cell proliferation assay (MTS assay; Promega, Madison, WI, USA) in triplicate or quadruplicate and expressed as the 50% inhibitory concentration (IC50), which was calculated using the linear relationship between the percentage inhibition and log concentration.

Establishment of trametinib-resistant cells (205T-R)

COLO-205 cells were cultured in medium containing trametinib at 10^{-3} nM, which can significantly suppress cell proliferation. When the cells showed viability, we gradually increased the concentration of trametinib until it reached at 2 nM. The entire induction period lasted ~6 months.

Organoid viability assay

Before the drug sensitivity assay, organoids were harvested as described above and disrupted with 2 ml TrypLE (Invitrogen) at 37 °C for ~6 min. Every 2 min, a visual check using a microscope was done to verify the size of the organoids. They were then suspended in wash medium and centrifuged at 4 °C 300 × *g* for 5 min. After removal of the supernatant, the pellets were reseeded as described above at a higher density than for usual passage (1:1 or less) in two wells in 12-well plates and cultured at 37 °C for 3 days. For the drug sensitivity assay, organoids were collected from Matrigel by treatment with 0.2% dispase II at 37 °C for 5 min. After washing with wash medium, the organoids were filtered using a 70 μm cell strainer (Greiner Bio One, Frichenhausen, Germany), and then organoids passed through the filter were filtered again using a 15 μm cell strainer (pluriSelect Life Science, Leipzig, Germany). The trapped organoids (between 15 and 70 μm in size) were collected with 4 ml of wash medium, counted, centrifuged and resuspended in organoid medium containing 10% Matrigel and serially diluted trametinib (10^{-5}, 10^{-4}, 10^{-3}, 10^{-2}, 10^{-1}, 0, 10 nM). Small organoids at a density of 1000 organoids/100 μl medium were then plated in each well of a 96-well repellent plate (Greiner Bio One) and cultured at 37 °C for 3 days. After the treatment, 100 μL of Cell Titer-Glo® 3D Cell Viability Assay Kit (Promega) was added to each well. The contents were vigorously mixed on a plate shaker for 5 min, incubated at room temperature for 25 min, transferred to a white microwell plate (Nunc, Roskilde, Denmark) and the luminescence was measured using a Fluoroskan Ascent FL (Thermo Fisher Scientific).

Western blotting

Western blotting was performed as described previously [16]. Before lysis, organoids were collected in ice-cold PBS. Cells or organoids were lysed on ice for 20 min in SDS-modified RIPA buffer containing protease and phosphatase inhibitor cocktails (cOmplete Mini; Roche Diagnostics, Mannheim, Germany) (PhosSTOP EASYpack; Roche Diagnostics), and then centrifuged at 4 °C 15,000 *rpm* for 20 min. The resulting cell lysates (20 μg each) were boiled with Laemmli sample buffer and subjected to

SDS-PAGE. The samples were transferred to a polyvinylidene difluoride membrane (Merk Millipore, Darmstadt, Germany), which was blocked for 1 h in Block Ace (DS Pharma, Osaka, Japan) at room temperature, then incubated overnight at 4 °C with primary antibodies against pERK1/2 (T202/Y204, 1:2000, Cat#4370, Cell Signaling Technology, Danvers, MA, USA), pS6 (S235/S236, 1:2000, Cat#4858, Cell Signaling Technology), pAKT (S437, Cat#4060, Cell Signaling Technology), ERK (1:2000, Cat #9102, Cell Signaling Technology), S6 (1: 2000, Cat#2217, Cell Signaling Technology), and GAPDH (1:1000, Cat#sc32233, Santa Cruz Biotechnology, Santa Cruz, CA, USA). After washing with 1 × TBS containing 0.1% Tween 20, the membranes were incubated for 1 h at RT with appropriate secondary antibodies, followed by rewashing. Finally, the signals were detected using an ECL Western blotting analysis system (GE Healthcare, Piscataway, NJ, USA) in accordance with the manufacturer's instructions. For detection of pERK, pS6 and GAPDH, we performed two or three independent Western blots, and representative data are shown. To verify the impact of trametinib treatment on the level of pERK or pS6, we performed statistical analysis using the results from three independent experiments at trametinib concentrations of 0 μM and 1.0 μM (cell lines) or 0.1 nM (organoids). The band intensities were quantified using Image J software (National Institute of Health, USA). We detected tERK, tS6 and pAKT in one or two Western blots, and representative data are shown.

Xenograft model

A total of 1×10^7 cells or ~8×10^4 small organoids suspended in 200 μl of OPTI-MEM (Thermo Fisher Scientific) were injected subcutaneously into the left flank of 7-week-old male NOD-SCID mice (Charles River Laboratories Japan). To determine the effect of MEK inhibition on pS6 expression, the mice at 4 weeks after injection were orally administered trametinib (3 mg/kg) dissolved in 200 μl of vehicle (0.5 w/v% Methyl Cellulose 400 Solution, Wako, Tokyo, Japan) or an equal volume of vehicle. Six hours after oral administration, the tumors were resected and subjected to immunohistochemical analysis. To determine the efficacy of trametinib on the xenografts from C3, the mice were divided into two groups 4 weeks after injection and then orally administered trametinib (3 mg/kg/day, 21 consecutive days) dissolved in 200 μl of vehicle or an equal volume of vehicle only. The experiment was performed one time with six replicates. Tumor volume was calculated once every 4 days using the formula: (width × length × height)/2. Tumor volume data are presented as the mean tumor volume ± SD, and were analyzed by Student's *t* test. All protocols for animal studies were approved by the animal ethics committee at Oita University (Approval No 182011).

Immunohistochemistry

We performed immunohistochemistry on paraffin-embedded blocks of xenografted tumor tissues using rabbit polyclonal antibodies against pERK(T202/Y204, 1:100) and pS6 (S240/244, 1:400, Cat#5364, Cell Signaling Technology), as described previously [4]. Briefly, after antigen retrieval and inactivation of endogenous peroxidase, tissue sections were blocked with 2.5% horse serum (ImmPRESS reagent kit; Vector Laboratories Inc., Burlingame, CA, USA) at RT for 30 min and then incubated at 4 °C overnight with antibodies against pERK and pS6 diluted in SignalStain Antibody Diluent (Cell Signaling Technology). After washing with PBS, the sections were incubated at RT for 30 min with peroxidase-conjugated horse anti-rabbit Ig (ImmPRESS reagent kit; Vector Laboratories Inc.). Peroxidase activity was detected using ImmPACT DAB Peroxidase Substrate (Vector Laboratories Inc.). For counting of pS6-positive cells, three to six representative images captured with a ×40 objective from each specimen were studied by a single experienced investigator. A total of at least 500 cells were counted in each xenograft.

Immunocytochemistry

Organoids cultured for 3 days were transferred to a 96-well glass-bottomed plate (EZ View culture plate; Iwaki, Shizuoka, Japan) and treated with DMSO or 1 nM trametinib for 24 h. Subsequently, the organoids were fixed with 4% PFA for 30 min and gently washed with 1 × PBS three times. They were then permeabilized with 0.5% Triton X-100/ PBS for 20 min, blocked with Block Ace (DS Pharma) in 0.05% Tween20/TBS for 1 h at room temperature and incubated overnight at 4 °C with a primary antibody against pS6 (S240/244) diluted 1:400. Subsequently, the organoids were washed with 0.05% Tween20/TBS three times and incubated with a secondary antibody (Alexa Fluor R488, 1:1000) and DAPI (diluted 1:1000) at RT for 2 h. After washing, images were captured using BZ-9000 or BZ-X800 (Keyence, Osaka, Japan). For quantitative analysis, we used images captured by the Sectioning Module of BZ-X800. At least six fields viewed with a ×40 objective (including a total of at least 12 organoids) were used for each group for quantification of the stained area by Image J software. The pS6-positive area was normalized by the DAPI-stained area.

Statistical analysis

The two-sided Student's *t* test was used to analyze differences in experiments (cell viability assays ($n = 3$ or 4), Western blotting ($n = 3$) and immunocytochemistry (6–9 fields in one group)). Data are reported as mean values ± SD. Differences at $p < 0.05$ were considered statistically significant.

Results

Sensitivity to trametinib is associated with the change in pS6 after trametinib treatment in CRC cell lines

We used nine CRC cell lines, composed of four KRAS-mutated cell lines and three BRAF-mutated cell lines and two cell lines without RAS/RAF mutations (Fig. 1a). First, we investigated their sensitivity to trametinib, which is an allosteric MEK inhibitor and blocks the RAS/MEK/ERK signaling pathway. We divided these cell lines into sensitive (COLO-205, WiDR, HCC-56, HCT-116) and resistant (COLO-320, CW-2, SUN-C2A, SUN-1033, SNU-C5) groups at a cut off value of 0.1 μM (Fig. 1b). Consistent with previous studies showing that cell lines with RAS or BRAF-oncogenic mutations are more sensitive to trametinib [17, 18], 4 of 7 CRC cell lines harboring RAS/BRAF mutation showed high sensitivity to MEK inhibition.

Previously, we had found that the change in pS6 after MEK inhibition was significantly associated with sensitivity to MEK inhibition in 48 GC cell lines [4]. To determine whether this is also the case in CRC cells, we used Western blotting to investigate changes in the phosphorylation levels of ERK and S6 after trametinib treatment (Fig. 1c). The level of pERK in all cell lines was effectively reduced by trametinib treatment (Fig. 1c), and no significant relationship was observed between the changes in pERK levels and trametinib sensitivity (Pearson's $r = 0.39$, $p = 0.301$, Fig. 1d right). On the other hand, decreases in the levels of pS6 were observed specifically in sensitive cells after MEK inhibition (Fig. 1c), and the ratios of the decrease were significantly related to trametinib sensitivity (Pearson's $r = 0.91$, $p < 0.001$, Fig. 1d left). We additionally investigated the sensitivity and pS6 response for MEK inhibition using another MEK inhibitor, PD0325901, and the significant relationship was also observed (Fig. S1).

To further confirm the relationship between the change in pS6 and sensitivity to trametinib, we established a cell line with acquired trametinib resistance (205T-R) using a sensitive cell line, COLO-205, through culture with increasing concentrations of trametinib over a period of ~6 months (Fig. 2a). The basal phosphorylation level of ERK was lower in 205T-R cells than in COLO-205 (Fig. S2), suggesting that 205T-R cells might become independent from the RAS-RAF-MEK-ERK pathway through activation of an alternative pathway. Indeed, the growth of 205T-R was slower than that of COLO-205 (Fig. S2). To investigate the difference in sensitivity to trametinib between COLO-205 and 205T-R cells, we optimized the doses of trametinib for the viability assay and used the same doses to compare the effects of trametinib treatment on pS6 in these cell lines. We confirmed by MTS assay that 205T-R cells were more resistant than the parental COLO-205 cells (Fig. 2b). As shown in Fig. 2c, pS6 was less affected by this treatment in 205T-R than in COLO-205. Thus, the close correlation between pS6 reduction and trametinib sensitivity suggested that the change in pS6 after MEK inhibition might predict the sensitivity of CRC cells to trametinib. We also established xenograft models using cell lines with in vitro sensitivity (COLO-205) and acquired resistance (205T-R). There was no obvious difference in histology between the xenografts of COLO-205 and 205T-R (Fig. S2). As shown in Fig. 2d, we found that a single treatment with trametinib (3 mg/kg) for 6 h suppressed pS6 as well as pERK in sensitive COLO-205 xenografts. In contrast, treatment with trametinib did not affect the level of pS6 in resistant 205T-R xenografts. Although the number of xenograft models was limited, these results suggested that the predictive change in pS6 might also be detectable in vivo.

Sensitivity of patient-derived CRC organoids to trametinib treatment

Our data for CRC cell lines suggested that it would be possible to distinguish trametinib-sensitive CRC cells by comparison of pS6 in the presence and absence of trametinib. To develop a preclinical model for CRC patients, we established ten CRC organoids from patients with advanced CRC (Table 1, Fig. 3a). The S6 phosphorylation levels in these CRC organoids were detectable by immunofluorescence staining (Fig. 3a left), and interestingly, the levels in the various clinical tumor samples tended to be similar (Fig. 3a right), suggesting that S6 activity in the primary tumor was recapitulated in the CRC organoids. Among the ten CRC organoids, six had a mutation in KRAS, one had a mutation in NRAS and one had a mutation in BRAF (Fig. 3b). To investigate their sensitivity to trametinib treatment, we performed the Cell Titer-Glo® 3D Cell Viability Assay using CRC organoids after 72 h of MEK inhibition. We optimized the doses of trametinib for the organoid viability assay to demonstrate the differences in sensitivity among the organoids. Similarly to other studies [19, 20], the sensitivities of organoids cultured under 3D conditions tended to be higher than those cultured under 2D conditions. The relative organoid viabilities and the corresponding IC50s resulting from MEK inhibition varied among the organoids (Fig. 3c, Fig. S3). Among the 7 CRC organoids harboring RAS or BRAF mutation, 2 were highly sensitive to trametinib; 2 of 3 CRC organoids without RAS or BRAF mutation were also sensitive to trametinib (Fig. 3c). These results suggested that a subset of patient-derived CRC organoids had high sensitivity to trametinib, regardless of their RAS/BRAF mutation status.

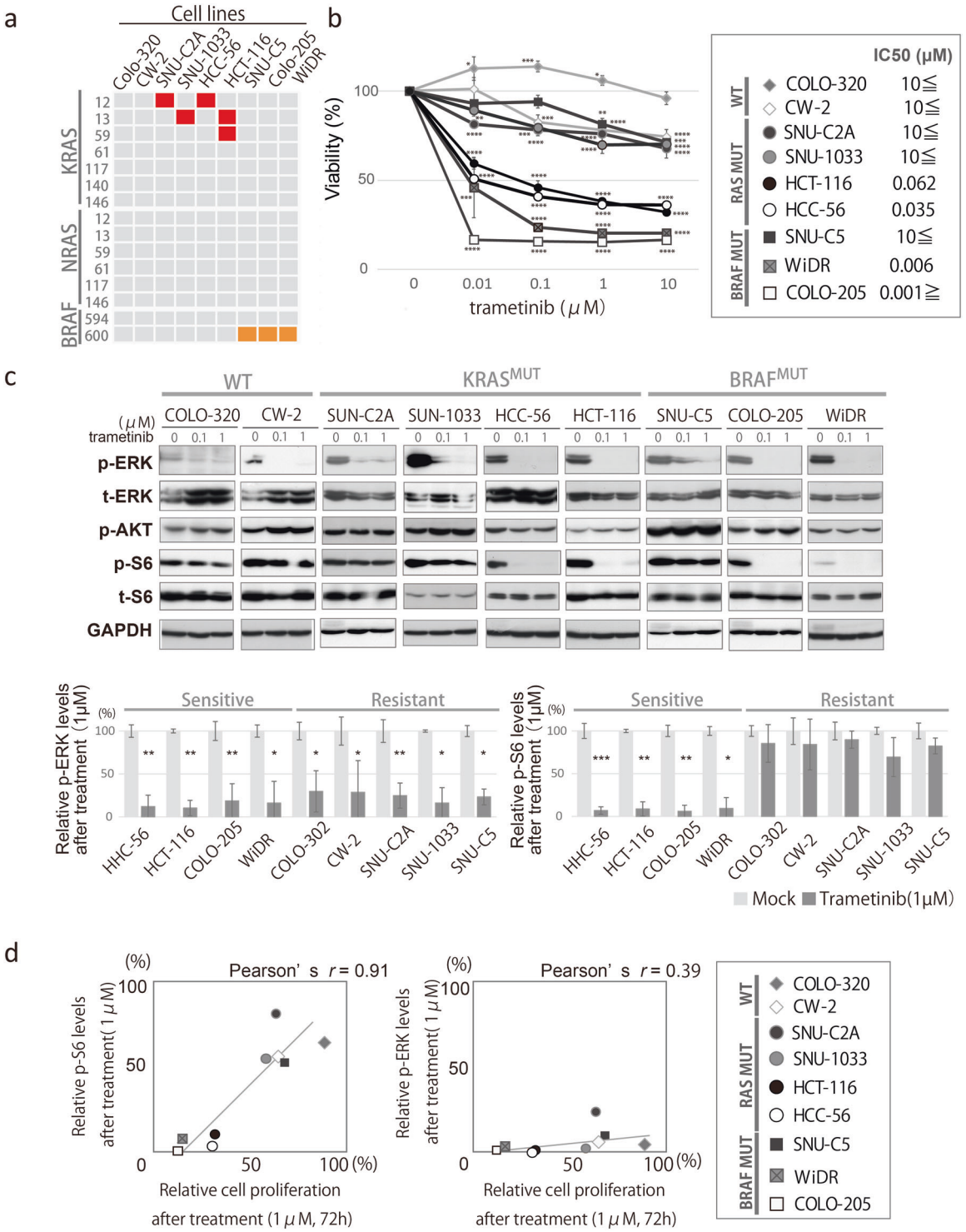

Fig. 1 Suppression of pS6 after MEK inhibition is related to sensitivity to MEK inhibition in a subset of RAS/BRAF mutant CRC cell lines. a The mutation status of RAS/BRAF in 9 CRC cell lines. **b** CRC cell lines were treated with increasing doses of trametinib for 3 days, and the cell viabilities and IC50 values were determined by MTS assay. The mean differences between samples with and without MEK inhibitor were analyzed statistically by Student's *t* test ($n = 4$). $^{*}p < 0.05$, $^{**}p < 0.01$, $^{***}p < 0.001$, $^{****}p < 0.0001$. **c** Sensitive (HCC-56, HCT-116, COLO-205,WiDR) or resistant (COLO-320, CW-2, SNU-C2A, SNU-1033, SNU-C5) CRC cell lines were treated with DMSO or trametinib (0.1 and 1 μM) for 24 h and then subjected to Western blotting using antibodies against pERK, tERK, pS6, tS6, pAKT, and GAPDH (upper panel). The band intensities of pERK and pS6 with Mock or 1 μM trametinib treatment in Western blots were analyzed statistically (lower panel). **d** The correlation between relative cell proliferation after trametinib treatment (1 μM, 72 h) and pS6 or pERK levels after trametinib treatment (1 μM, 24 h).

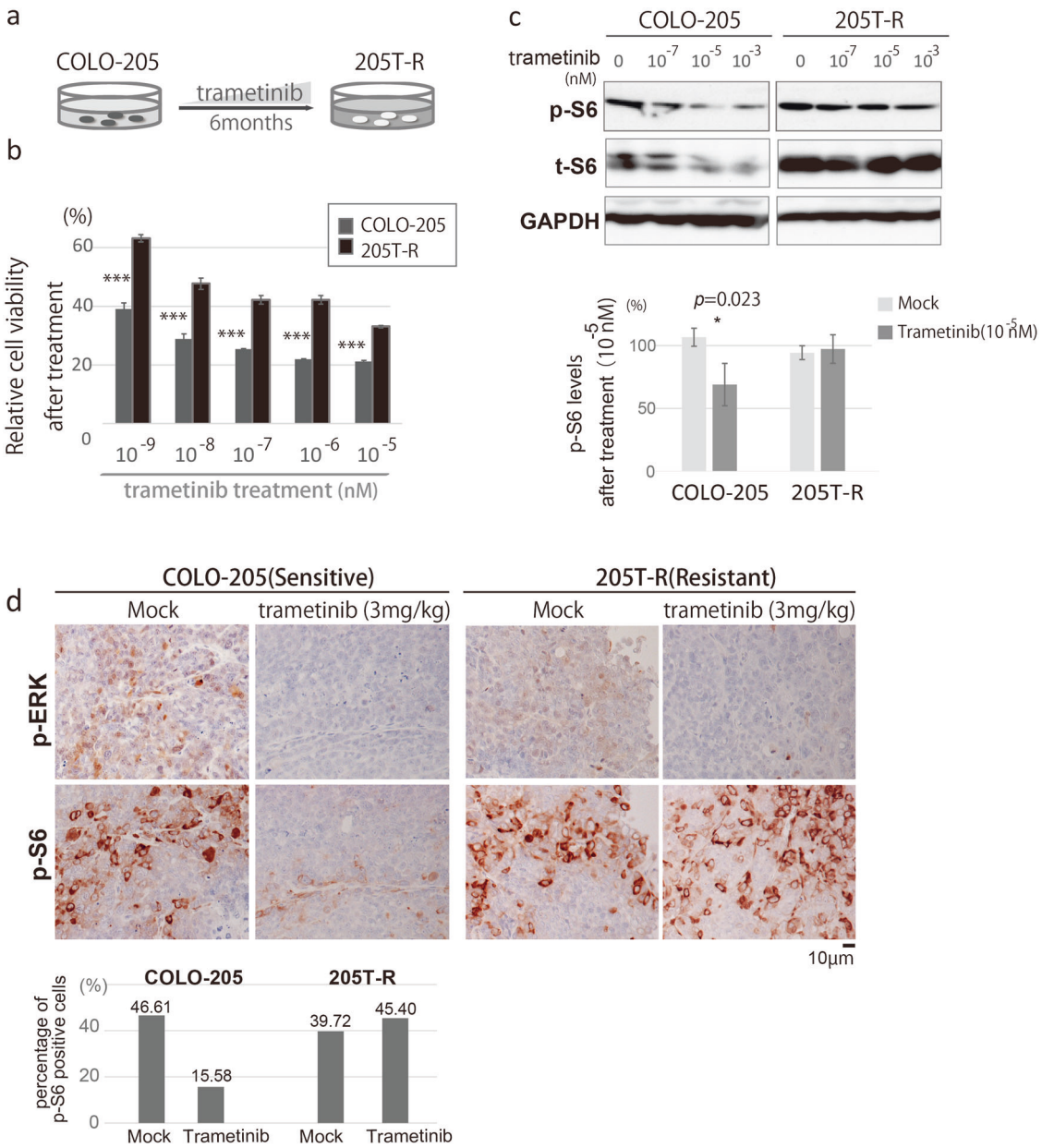

Fig. 2 Correlation between efficacy of MEK inhibition and pS6 response to treatment in CRC cells with acquired trametinib resistance. a 205T-R cells with acquired trametinib resistance were established by culturing COLO-205 cells with increasing concentrations of trametinib over 6 months. **b** and **c** Relative viability and pS6 levels after trametinib treatment at the indicated concentrations in COLO-205 and 205T-R cells. The mean differences between samples with and without MEK inhibitor were analyzed statistically by Student's *t* test ($n = 3$). *$p < 0.05$, **$p < 0.01$, ***$p < 0.001$, ****$p < 0.0001$. Independent experiments were performed twice with similar results, and representative data are shown. **d** Tumor xenografts established from COLO205 or resistant 205T-R cells were sacrificed 6 h after treatment with a single dose of vehicle (Mock) or trametinib (3 mg/kg) ($n = 1$ in each treatment). Representative images of immunohistochemistry using antibodies against pERK and pS6 are shown. Two independent experiments were performed with similar results, one of which was used to calculate the percentage of pS6 cells.

Relationship between trametinib sensitivity and change in pS6 after trametinib treatment in patient-derived CRC organoids

Next, to further investigate whether the change in pS6 is also related to trametinib sensitivity in CRC organoids, we performed Western blotting to investigate changes in the phosphorylation levels of ERK and S6 in patient-derived CRC organoids (sensitive, $n = 4$; resistant, $n = 6$) (Fig. 4a). Unlike the pERK levels in the cell line experiments, some resistant organoids (C2, C7, C13) showed stable pERK levels after trametinib treatment (Fig. 4a), although the

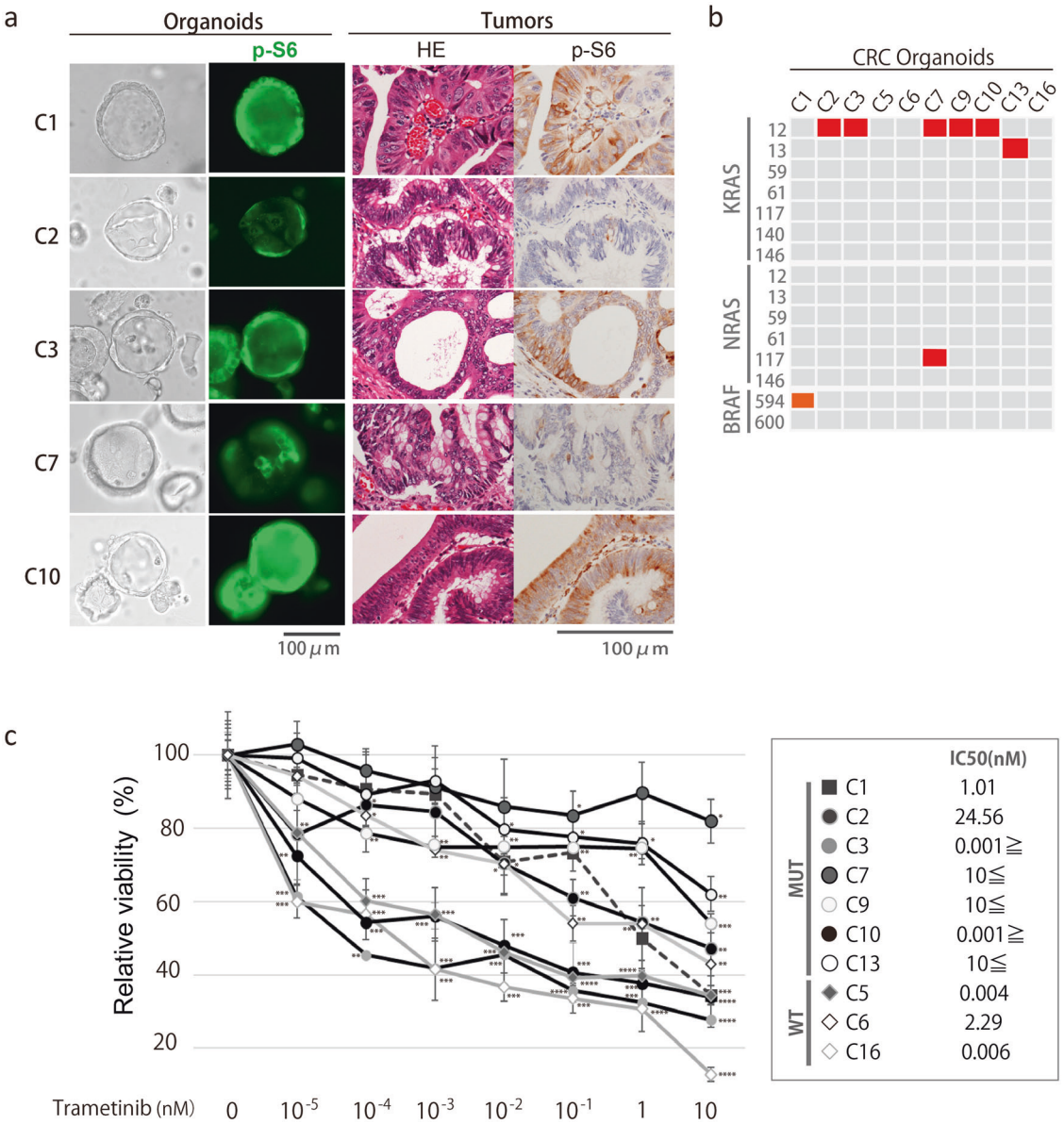

Fig. 3 Establishment of patient-derived CRC organoids. a Representative bright-field and immunofluorescence images of pS6 in CRC organoids (left panel), and hematoxylin-eosin staining and immunohistochemistry for pS6 in primary tissues, from which CRC organoids were originally derived (right panel). **b** The mutation status of RAS/BRAF in CRC organoids. **c** Viabilities and IC50s of CRC organoids 72 h after treatment with trametinib at 10^{-5} to 10 nM were determined using the 3D-Glo assay. The mean differences between samples with and without MEK inhibitor were analyzed statistically by Student's *t* test ($n = 3$). *$p < 0.05$, **$p < 0.01$, ***$p < 0.001$, ****$p < 0.0001$. Two independent experiments were performed with similar results, and representative data are shown. Another experiment is shown in Fig. S3.

change was not significantly associated with sensitivity to trametinib (Pearson's $r = 0.56$, $p = 0.09$, Fig. 4b left). Meanwhile, striking decreases in the levels of pS6 were observed in sensitive CRC organoids after MEK inhibition (Fig. 4a) and these were significantly correlated with trametinib sensitivity (Pearson's $r = 0.78$, $p = 0.007$, Fig. 4b right). The specific reduction of pS6 by MEK inhibition in trametinib-sensitive CRC organoids (C3, C10, C16) was found to be detectable by fluorescence staining (Fig. 4c). Moreover, using the xenograft model, we found that a single treatment with trametinib (3 mg/kg) for 6 h suppressed pS6 in a sensitive organoid xenograft (C3) but did not affect the level of pS6 in resistant organoid xenografts (C1 and C7) (Fig. 4d). Consistent with the in vitro results (Fig. 3c), C3-derived xenografts were sensitive to trametinib (Fig. S4). These results suggested that, in combination with patient-derived organoids, the change in pS6 could be a useful biomarker for prediction of sensitivity to trametinib.

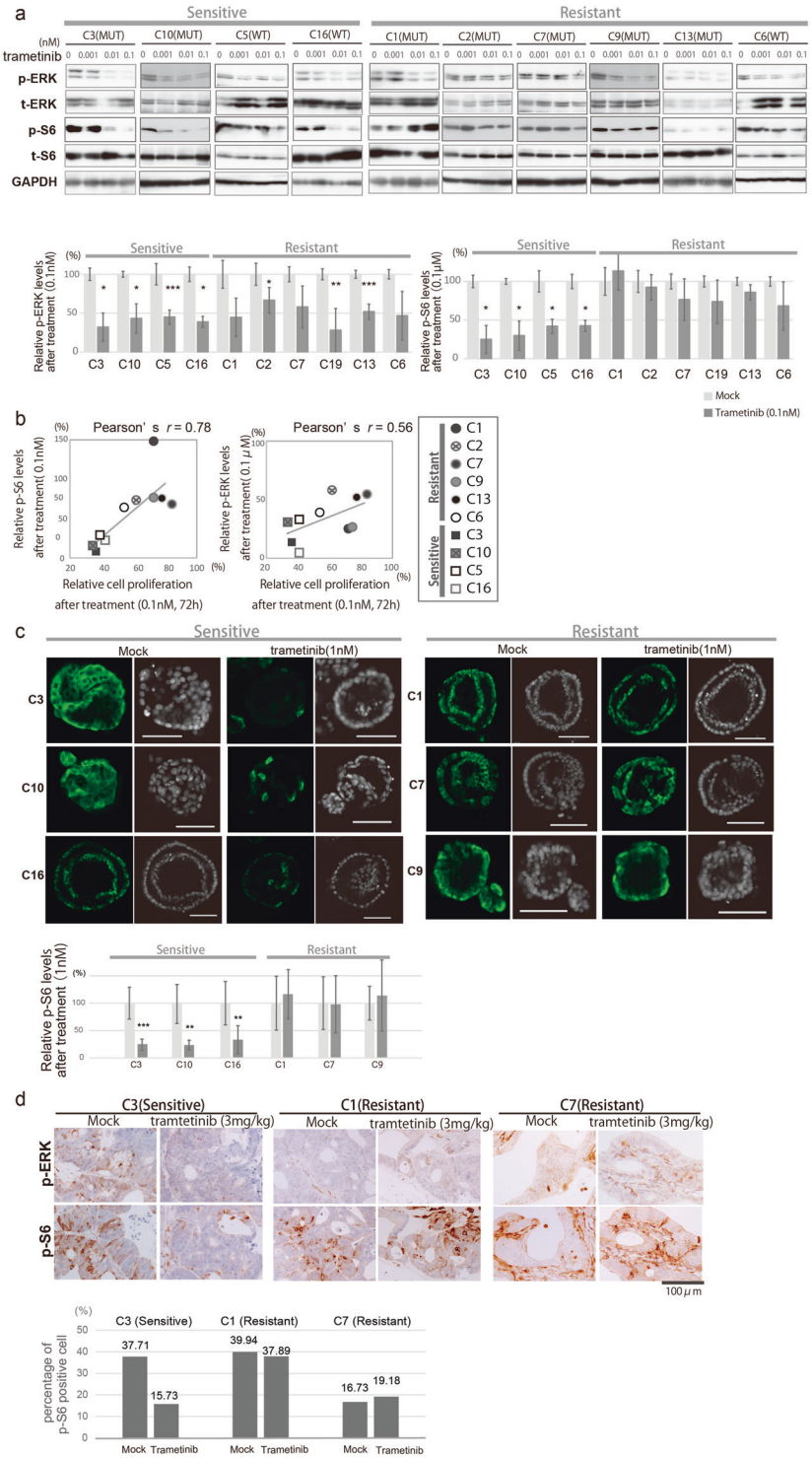

Fig. 4 Response of the pS6 level after MEK inhibition is also related to trametinib sensitivity in CRC organoids. **a** Sensitive (C3, C10, C5, C16) and resistant (C1, C2, C7, C9, C13, C6) CRC organoids were treated with DMSO or trametinib (0.001, 0.01 and 0.1 nM) for 24 h and then subjected to Western blotting using antibodies against pERK, tERK, pS6, tS6 and GAPDH. The band intensities of pERK and pS6 with Mock or 0.1 nM trametinib in Western blots were analyzed statistically. **b** Correlations between viabilities after trametinib treatment (0.1 nM, 72 h) and pS6 or pERK levels after trametinib treatment (0.1 nM, 24 h). **c** Trametinib-sensitive (C3, C10, C16) or resistant (C1, C7, C9) organoids were treated with DMSO or trametinib (1 nM) for 24 h and subjected to immunofluorescence for pS6. Similar results were obtained in two independent experiments for each organoid, one of which was subjected to quantitative analysis of the stained area and is shown in the graphs (lower panel). **d** Tumor xenografts established from sensitive (C3) and resistant (C1 and C7) organoids were sacrificed 6 h after treatment with a single dose of vehicle (Mock) or trametinib (3 mg/kg) ($n = 1$ in each treatment) and subjected to immunohistochemistry using antibodies against pERK and pS6. Two independent experiments were performed with similar results, one of which was used to calculate the percentage of pS6 cells.

Discussion

In general, genomic alterations tend to be utilized as predictors of responsiveness to molecular- targeted drugs. In the present study, we showed that the change in pS6 after MEK inhibition was well correlated with responsiveness to trametinib among CRC cell lines and patient-derived CRC organoids. Our data suggest three potential avenues for CRC therapy. First, MEK-targeted therapy might be applicable for patients with RAS/RAF/ERK pathway-dependent CRC. Currently, CRC patients with RAS or BRAF mutation are excluded from EGFR-targeted therapy, which is one of the

standard treatments for CRC, because mutant KRAS or BRAF activate downstream of EGFR activity independently from EGFR activation [21–23]. Furthermore, such patients who are excluded from EGFR-targeted therapy also do not receive MEK-targeted therapy, even though the RAS/RAF/ERK pathway is assumed to be activated in CRC with RAS mutation. This is largely based on the results of clinical trials involving patients with RAS-mutated CRC, for whom no superiority of MEK-targeted therapy has yet been proven relative to conventional chemotherapies [12–14]. In fact, we also showed that among CRC cell lines and organoids with RAS or RAF mutation, only some were sensitive to trametinib whereas others were resistant. These clinical trials and our present data suggest that it would be reasonable to use biomarkers other than RAS or RAF mutation status for prediction of responsiveness to MEK inhibition. Therefore, by combining our predictive system with the change in pS6 after MEK inhibition, MEK inhibitors might have potential clinical applicability for a proportion of patients with CRC harboring RAS or RAF mutation, who currently are excluded from EGFR-targeted therapies. In addition, our predictive system would also be applicable to combination therapies with MEK, BRAF and/or EGFR-targeted agents, which were recently reported to be more effective for BRAF-mutated metastatic CRC than conventional chemotherapy [24–26]. To test our proposal, further studies with larger numbers of organoids from CRC patients will be required.

Secondly, we found that reduction of pS6 levels in response to short term-trametinib treatment was well correlated to the trametinib sensitivities in CRC organoids, suggesting that reduction of pS6 levels could be a useful predictive biomarker for trametinib efficacy. Currently ATP-based cell viability assay is mainly used to determine the efficacy of drugs in most studies using organoids [27, 28]. However, this assay still has some limitations. For example, it is costly and time-consuming to obtain a sufficient amount of organoids [15]. Moreover, the heterogeneity of organoid culture leads to inter- and intra-assay variability in the size and growth speed of individual organoids, thus limiting its applicability to drug screening [8, 29, 30]. To reduce this variation, certain complicated procedures are needed, such as filtration to make the organoid size more uniform (see "Organoid viability assay" in Materials and Methods) and mathematical modeling to correct for variations in growth speed [31, 32]. In the present study, we showed that reduction of pS6 expression in response to drug treatment was detectable by immunocytochemistry, which would be advantageous in reducing the amount of organoids required and making organoid size irrelevant. Intracellular pS6 levels in organoid cultures appeared to be correlated with those in the primary tumor tissues from which they were originally derived (Fig. 3a). Furthermore, there was a correlation between the pS6 change resulting from trametinib treatment and the degree of sensitivity in the xenograft model. These results suggest that the intracellular phosphorylation level of S6 is mainly regulated by intrinsic signaling pathways and that the impact of trametinib treatment might be greater than that of the extracellular environment, although phosphorylation of S6 is known to be regulated by multiple factors, such as nutritive and growth factors, in the milieu around growing tumors [33–35]. This hypothesis requires further verification, since the number of xenograft models we used was limited. In contrast to the changes in pS6 observed in organoids, those in pERK, which also showed a tendency to be associated with sensitivity, were difficult to detect in organoids by immunocytochemistry using our system (data not shown). Thus, immunostaining-based detection of pS6 in organoids with or without trametinib treatment could be a simple and robust diagnostic approach with potential advantages over conventional cell viability assays for prediction of sensitivity to trametinib.

Finally, although the mechanism by which trametinib treatment decreases the phosphorylation of S6 in trametinib-sensitive but not -resistant CRC remains largely unknown, our results suggest the importance of maintaining the S6 phosphorylation level during CRC cell proliferation. Ribosomal protein S6 is considered to be one of the important downstream effectors of the AKT/mTOR signaling pathway, which plays a crucial role in cancer cell survival. Some recent studies have suggested that compensatory activation of the AKT/mTOR signal causes to resistance to MEK inhibition in cancer cells [36]. We also investigated the AKT phosphorylation response after treatment of MEK inhibition, but AKT activity was not associated with sensitivity to MEK inhibition in this study (Fig. 1c), as had also been the case in our previous study [4]. These results suggest that S6 activity is regulated by certain molecule(s) after MEK inhibition, with little relation to AKT activity. Further studies to investigate the association between sensitivity to MEK inhibition and the response in pS6 would likely lead to improvement in the clinical outcome of trametinib treatment for patients, as well as clarifying the mechanism of CRC progression.

Data availability

The data that support the findings of this study are available from the corresponding authors, upon reasonable request.

Acknowledgements We would like to thank Ms Mami Kimoto for their excellent assistance with experiments. We are also grateful to Hans Clevers, Tomohiro Mizutani, Else Driehuis and Stieneke van den Brink for critical advice on organoid experiments.

Author contributions Conceptualization: YH, YT; Formal analysis and investigation: YH, YK; Writing—original draft preparation: YH, YT; Writing—review and editing: DK, SK, NH, CN, TU, TH, KM,

KH, TO, MK; Funding acquisition: YH; Resources: TH, TA, YU, HS, TE; Supervision: MI, MM, KM. All authors have approved the final version of the paper.

Funding This work was supported at the Discretion of the President of Oita University (2019) and partly by JSPS KAKENHI Grant Number 18K15283.

Compliance with ethical standards

Conflict of interest The authors declare no competing interests.

Ethical approval This study was approved by the ethics committee of Oita University Faculty of Medicine (approval number: 1541).

Publisher's note Springer Nature remains neutral with regard to jurisdictional claims in published maps and institutional affiliations.

References

1. Ciriello G, Miller ML, Aksoy BA, Senbabaoglu Y, Schultz N, Sander C. Emerging landscape of oncogenic signatures across human cancers. Nat Genet. 2013;45:1127–33.
2. Dancey JE, Bedard PL, Onetto N, Hudson TJ. The genetic basis for cancer treatment decisions. Cell. 2012;148:409–20.
3. Hyman DM, Taylor BS, Baselga J. Implementing Genome-Driven Oncology. Cell. 2017;168:584–99.
4. Hirashita Y, Tsukamoto Y, Yanagihara K, Fumoto S, Hijiya N, Nakada C, et al. Reduced phosphorylation of ribosomal protein S6 is associated with sensitivity to MEK inhibition in gastric cancer cells. Cancer Sci. 2016;107:1919–28.
5. Sato T, Stange DE, Ferrante M, Vries RG, Van Es JH, Van den Brink S, et al. Long-term expansion of epithelial organoids from human colon, adenoma, adenocarcinoma, and Barrett's epithelium. Gastroenterology. 2011;141:1762–72.
6. Vlachogiannis G, Hedayat S, Vatsiou A, Jamin Y, Fernandez-Mateos J, Khan K, et al. Patient-derived organoids model treatment response of metastatic gastrointestinal cancers. Science. 2018;359:920–6.
7. Saito Y, Muramatsu T, Kanai Y, Ojima H, Sukeda A, Hiraoka N, et al. Establishment of Patient-Derived Organoids and Drug Screening for Biliary Tract Carcinoma. Cell Rep. 2019;27:1265–76.e1264.
8. Kondo, J & Inoue, M. Application of Cancer Organoid Model for Drug Screening and Personalized Therapy. Cells. 2019;8:470.
9. Cunningham D, Humblet Y, Siena S, Khayat D, Bleiberg H, Santoro A, et al. Cetuximab Monotherapy and Cetuximab plus Irinotecan in Irinotecan-Refractory Metastatic Colorectal Cancer. N Engl J Med. 2004;351:337–45.
10. Karapetis CS, Jonker DJ, O'Callaghan CJ, Tu D, Tebbutt NC, et al. K-ras Mutations and Benefit from Cetuximab in Advanced Colorectal Cancer. N Engl J Med. 2008;23:1757–65.
11. Sandhu J, Lavingia V, Fakih M. Systemic treatment for metastatic colorectal cancer in the era of precision medicine. J Surg Oncol. 2019;119:564–82.
12. Korphaisarn K, Kopetz S. BRAF-Directed Therapy in Metastatic Colorectal Cancer. Cancer J. 2016;22:175–8.
13. Wagner S, Vlachogiannis G, De Haven Brandon A, Valenti M, Box G, Jenkins L, et al. Suppression of interferon gene expression overcomes resistance to MEK inhibition in KRAS-mutant colorectal cancer. Oncogene. 2019;38:1717–33.
14. Cho M, Gong J, Frankel P, Synold TW, Lim D, Chung V, et al. A phase I clinical trial of binimetinib in combination with FOLFOX in patients with advanced metastatic colorectal cancer who failed prior standard therapy. Oncotarget. 2017;8:79750–60.
15. van de Wetering M, Francies HE, Francis JM, Bounova G, Iorio F, Pronk A, et al. Prospective derivation of a living organoid biobank of colorectal cancer patients. Cell. 2015;161:933–45.
16. Moriyama M, Tsukamoto Y, Fujiwara M, Kondo G, Nakada C, Baba T, et al. Identification of a novel human ankyrin-repeated protein homologous to CARP. Biochem Biophys Res Commun. 2001;285:715–23.
17. Jing J, Greshock J, Holbrook JD, Gilmartin A, Zhang X, McNeil E, et al. Comprehensive predictive biomarker analysis for MEK inhibitor GSK1120212. Mol Cancer Ther. 2012;11:720–9.
18. Yeh JJ, Routh ED, Rubinas T, Peacock J, Martin TD, Shen XJ, et al. KRAS/BRAF mutation status and ERK1/2 activation as biomarkers for MEK1/2 inhibitor therapy in colorectal cancer. Mol Cancer Ther. 2009;8:834–43.
19. Jacobi N, Seeboeck R, Hofmann E, Schweiger H, Smolinska V, Mohr T, et al. Organotypic three-dimensional cancer cell cultures mirror drug responses in vivo: lessons learned from the inhibition of EGFR signaling. Oncotarget. 2017;8:107423–40.
20. Pickl M, Ries CH. Comparison of 3D and 2D tumor models reveals enhanced HER2 activation in 3D associated with an increased response to trastuzumab. Oncogene. 2009;28:461–468.
21. Fang JY, Richardson BC. The MAPK signalling pathways and colorectal cancer. Lancet Oncol. 2005;6:322–7.
22. Lievre A, Bachet JB, Le Corre D, Boige V, Landi B, Emile JF, et al. KRAS mutation status is predictive of response to cetuximab therapy in colorectal cancer. Cancer Res. 2006;66:3992–5.
23. Di Nicolantonio F, Martini M, Molinari F, Sartore-Bianchi A, Arena S, Saletti P, et al. Wild-type BRAF is required for response to panitumumab or cetuximab in metastatic colorectal cancer. J Clin Oncol. 2008;26:5705–12.
24. Corcoran RB, Andre T, Atreya CE, Schellens JHM, Yoshino T, Bendell JC, et al. Combined BRAF, EGFR, and MEK Inhibition in Patients with BRAF(V600E)-Mutant Colorectal Cancer. Cancer Discov. 2018;8:428–43.
25. Kopetz S, Grothey A, Tabernero J. Encorafenib, Binimetinib, and Cetuximab in BRAF V600E-Mutated Colorectal Cancer. Reply. N Engl J Med. 2020;382:877–8.
26. Corcoran RB, Atreya CE, Falchook GS, Kwak EL, Ryan DP, Bendell JC, et al. Combined BRAF and MEK Inhibition With Dabrafenib and Trametinib in BRAF V600-Mutant Colorectal Cancer. J Clin Oncol. 2015;33:4023–31.
27. Phan N, Hong JJ, Tofig B, Mapua M, Elashoff D, Moatamed NA, et al. A simple high-throughput approach identifies actionable drug sensitivities in patient-derived tumor organoids. Commun Biol. 2019;2:78.
28. Seidlitz T, Merker SR, Rothe A, Zakrzewski F, von Neubeck C, Grutzmann K, et al. Human gastric cancer modelling using organoids. Gut. 2019;68:207–17.
29. Zanoni M, Piccinini F, Arienti C, Zamagni A, Santi S, Polico R, et al. 3D tumor spheroid models for in vitro therapeutic screening: a systematic approach to enhance the biological relevance of data obtained. Sci Rep. 2016;6:19103.
30. Kim M, Mun H, Sung CO, Cho EJ, Jeon HJ, Chun SM, et al. Patient-derived lung cancer organoids as in vitro cancer models for therapeutic screening. Nat Commun. 2019;10:3991.
31. Harris LA, Frick PL, Garbett SP, Hardeman KN, Paudel BB, Lopez CF, et al. An unbiased metric of antiproliferative drug effect in vitro. Nat Methods. 2016;13:497–500.
32. Hafner M, Niepel M, Chung M, Sorger PK. Growth rate inhibition metrics correct for confounders in measuring sensitivity to cancer drugs. Nat Methods. 2016;13:521–7.
33. Guertin DA, Sabatini DM. Defining the role of mTOR in cancer. Cancer Cell. 2007;12:9–22.

34. Dyachok J, Earnest S, Iturraran EN, Cobb MH, Ross EM. Amino Acids Regulate mTORC1 by an Obligate Two-step Mechanism. J Biol Chem. 2016;291:22414–26.
35. Munoz-Cordero MG, Lopez F, Garcia-Inclan C, Lopez-Hernandez A, Potes-Ares S, Fernandez-Vanes L, et al. Predictive value of EGFR-PI3K-pAKT-mTOR-pS6 pathway in sinonasal squamous cell carcinomas. Acta Otorrinolaringol Esp. 2019;70:16–24.
36. Chen CH, Hsia TC, Yeh MH, Chen TW, Chen YJ, Chen JT, et al. MEK inhibitors induce Akt activation and drug resistance by suppressing negative feedback ERK-mediated HER2 phosphorylation at Thr701. Mol Oncol. 2017;11:1273–87.